



Ground motion simulation validation with explicit uncertainty incorporation for small-magnitude earthquakes

S.J. Neill, R.L. Lee & B.A. Bradley

University of Canterbury, Christchurch.

P.J. Stafford

Imperial College London, United Kingdom.

ABSTRACT

This study investigates the uncertainty of simulated earthquake ground motions for small-magnitude events (M_w 3.5 – 5) in Canterbury, New Zealand. 148 events were simulated with specified uncertainties in: event magnitude, hypocentre location, focal mechanism, high frequency rupture velocity, Brune stress parameter, the site 30-m time-averaged shear wave velocity (V_{s30}), anelastic attenuation (Q) and high frequency path duration. In order to capture these uncertainties, 25 realisations for each event were generated using the Graves and Pitarka (2015) hybrid broadband simulation approach. Monte-Carlo realisations were drawn from distributions for each uncertainty, to generate a suite of simulation realisations for each event and site. The fit of the multiple simulation realisations to observations were assessed using linear mixed effects regression to generate the systematic source, path and site effects components across all ground motion intensity measure residuals. Findings show that additional uncertainties are required in each of the three source, path, and site components, however the level of output uncertainty is promising considering the input uncertainties included.

1 INTRODUCTION

Ground-motion models (GMMs) are used to predict intensity measures (IM) from seismic events, and are a key part of the probabilistic seismic hazard analysis (PSHA) framework used for earthquake engineering design. Previously, the New Zealand Seismic Hazard Model, as well as other international equivalents, have used empirically derived ground motion models. However, over recent years there has been a trend towards developing site-specific physics-based ground motion simulation models. The continual advancement of high performance computing resources has enabled accurate simulations, with high resolutions for computing the physical phenomena of an earthquake fault rupture and wave propagation. These models are considered to have the potential for lower aleatory variability than traditional GMPEs, due to their use of

region and site-specific modelling which relies less on globally averaged parameter assumptions. Simulations also have the capability to generate synthetic data where recorded data may be lacking, such as engineering design-level events that are high magnitude and close proximity.

Simulation models are nominally deterministic, in that a single set of parameters will always produce the same result. In order to make simulations probabilistic, they must explicitly incorporate uncertainty. While some quantities in the simulation model used for this study are already specified stochastically (high frequency random phasing and random source slip distributions), no previous simulation validation studies (Lee et al. 2019; Graves et al. 2011; Somerville et al. 1991) have comprehensively incorporated uncertainty in simulations. This study has been conducted to address these limitations by explicitly including a number of parameter and model uncertainties associated with the source, path and site components of physics-based ground motion simulations. Figure 1 illustrates an example event and site for which the difference between response spectra results for a deterministic simulation and a probabilistic simulation can be compared. In the probabilistic case, added uncertainties are propagated through the simulation model to produce a distribution of realisations which provides a median and standard deviation value for each IM.

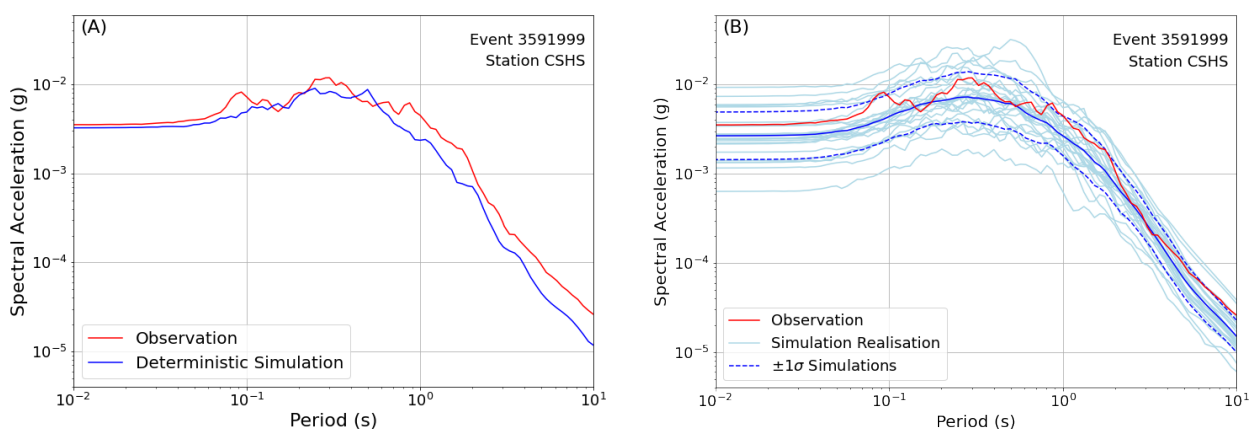


Figure 1: The response spectra for event 3591999 (Mw 4.9, Godley Head) and station CSHS observation and simulation. (A) Deterministic ground motion simulation. (B) Simulation with explicit uncertainty incorporation, producing IM realisations with an IM distribution and sigma.

In order to validate if the amount of uncertainty included in probabilistic ground motion simulations is appropriate for the uncertainty in observations, a unique framework for validating input uncertainties is required. Other ground motion simulation studies have used past-event observation data to validate the median ground motion and in some cases a linear mixed effects regression framework has been used to further decompose residuals (e.g. Lee et al. (2019)). But there are no instances of comprehensive validation of input uncertainties for ground-motion simulation models. A proposed framework for validating ground motion simulation uncertainty is included in Section 2.4, and the results from the proposed framework for a Canterbury region pilot study are presented in Section 3.

2 EARTHQUAKE EVENTS AND SIMULATION METHOD

2.1 Ground motion data

This study provides an initial examination of the parameter and model uncertainties in a ground motion simulation method used for a New Zealand context, focussing on small magnitude events in Canterbury. The dataset used includes observations for 148 small magnitude (Mw 3.5 – 5) events recorded at 42 stations, resulting in 1802 observed ground motions. Figure 2 illustrates these locations in the Canterbury region, which were also used to produce a simulation data set for the same records.

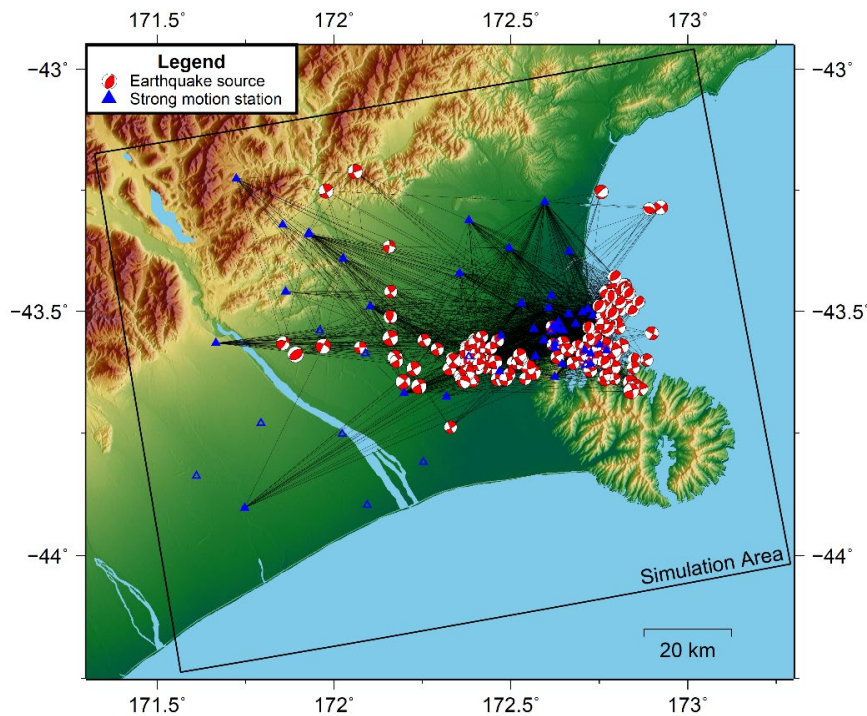


Figure 2: Map of the Canterbury region with the 148 event and 42 station locations considered in this study.

Small magnitude events were selected for this study due to the large amount of data, when compared with moderate or large magnitude events, which is useful for validation. This wealth in data allows statistical inferences to be made in the causal contributions to the overall output uncertainties. The use of small magnitude data also helps to simplify validation by reducing the number of uncertainties that should be considered. This is due to the applicability of simpler models with less parameters in the simulation process for these types of events. For instance, non-linear site effects can be discounted due to the small ground-motion amplitudes. A point source model can also be used in lieu of a finite fault for the event rupture, due to the relatively small rupture area to site recording distance ratio. The selection of the Canterbury region for this study has also been made in part due to the large amount of recently recorded ground motion data, as well as the availability of a rigorously validated velocity model (NZVM) in this region (Thomson et al. 2019; Lee et al. 2017), and prior ground-motion simulation validation studies that excluded consideration of simulation uncertainties (Lee et al. 2020).

2.2 Simulation method and crustal velocity model

The simulation method applied in this study utilises the hybrid broadband ground motion simulation approach developed by Graves and Pitarka (2010, 2015, 2016) with modifications from Lee et al. (2020). This method simulates low-frequency (LF; $f < 0.25\text{Hz}$) ground motions using a comprehensive physics-based approach and high-frequency (HF; $f > 0.25\text{Hz}$) ground motions using a simplified physics-based approach. The HF component is subsequently modified with an empirical amplification factor to account for local site effects and then merged with the LF component to produce a single broadband time series. The ground-motion simulations were performed within event-specific computational domains, an example of which the surface projection is shown in Figure 2. The 3D NZVM domain is used for solving the viscoelastic wave equation with the finite difference method, in order to calculate the ground motion's low frequency waveforms. Crustal seismic velocities were prescribed from the Canterbury Velocity Model (Thomson et al. 2019; Lee et al. 2017), with a spatial resolution of 0.4 km. An enforced minimum shear wave velocity of 500 m/s was used, which yields a maximum frequency of 0.25 Hz in the LF component. A time-step of $\Delta t =$

0.005 s was used to ensure numerical stability. A relatively large spatial resolution (0.4 km) was selected during this preliminary study to balance computational requirements while exploring parameter uncertainties. The intent is to reduce spatial resolution to 0.1 km in the future, consistent with prior work in the region (e.g. Lee et al. (2020)).

2.3 Uncertainties considered

The uncertainty input parameters are selected based on their contribution to the output uncertainty of the ground motion intensity measures (Neill et al. 2019). The uncertainty values of these input parameters are based on a review of the literature for each parameter, as well as in some cases, other independent measurements or calculations. For instance, the geographic location and depth uncertainties draw on data from Bannister et al. (2011) for a number of events, in order to further refine the location uncertainties for those events. Figure 3 outlines the chosen uncertainty parameters with their associated references (Eberhart-Phillips et al. 2010; Lee et al. 2017; Thomson et al. 2019; Graves 2018; Mai et al. 2005; Ristau 2008; Graves and Pitarka 2010; Taborda 2015; Foster et al. 2019; Lee et al. 2020; Graves and Pitarka 2016; Boore and Thompson 2014). The histograms in Figure 3 demonstrate the parameter distributions generated from 25 realisations for all the records considered, and their underlying parametric distributions are shown in red.

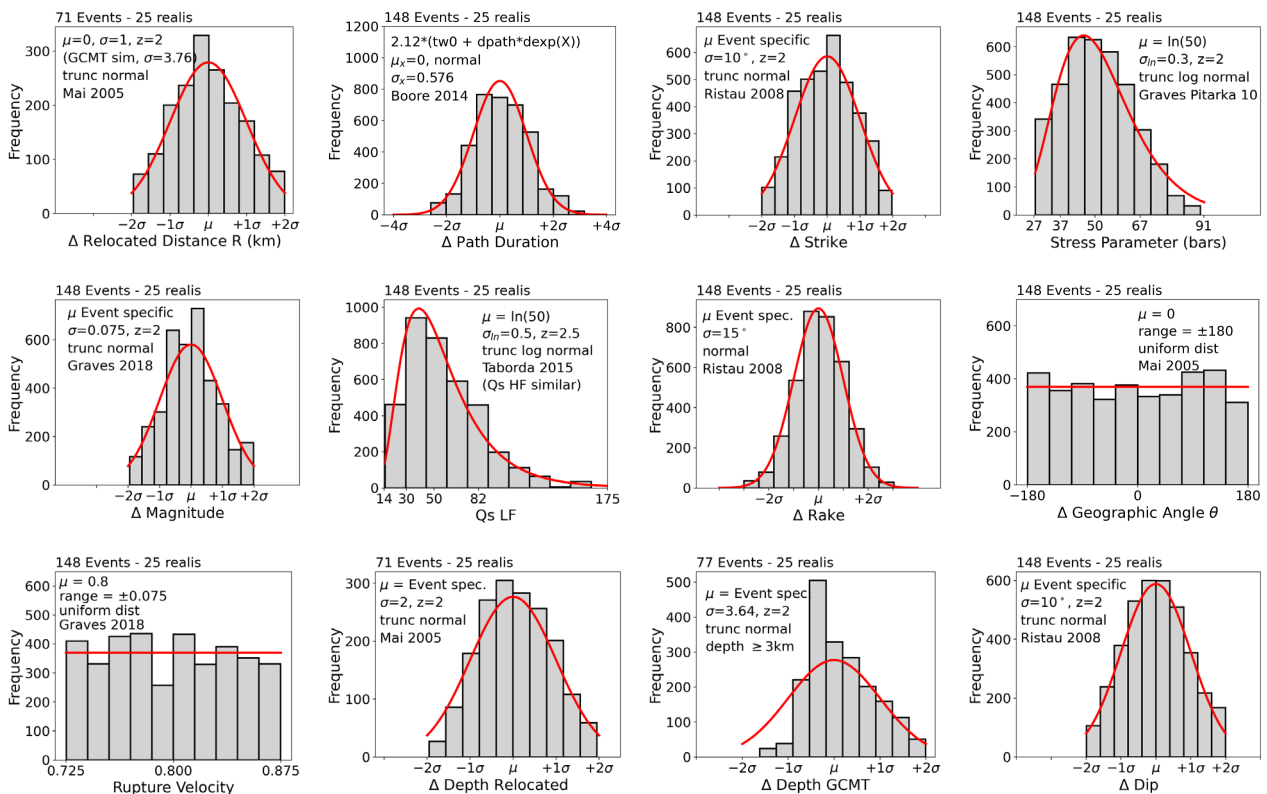


Figure 3: Uncertainty distributions used for parameter perturbations, representing 3700 simulations. The selected uncertainties are associated with the following source, path and site parameters: rupture velocity ratio, magnitude, the Brune stress parameter, path duration, geographic location, attenuation, strike, dip, rake, depth and site Vs30. ‘z’ is the number of standard deviations at which the distribution is truncated.

2.4 Validation method

In order to undertake validation of the simulated ground motions with incorporated uncertainty, the following intensity measures of engineering interest were used: PGA, pSA, CAV, AI, Ds575 and Ds595. These were calculated from the simulated and observed ground-motion waveforms, and then used to compute residuals (Δ^k) following Equation 1.

$$\Delta^k = \ln IM_{obs\ es} - \ln IM_{sim\ es}^k \quad (1)$$

where k, e, and s represent a given realisation, event and site respectively. IM_{obs} is the ground motion observation and IM_{sim} is the simulated ground motions for a single IM.

The residuals were partitioned through conducting a linear mixed effects regression across all events and all stations, in order to assess the systematic effects of the uncertainties. Equation 2 demonstrates how each realisation was partitioned in this way, with event and site identifiers treated as the random effects. An assessment was then made between the standard deviations for each realisation, component and all random effects (τ^k , ϕ_{S2S}^k , ϕ_{SS}^k), with the standard deviations for each component, random effect and all realisations ($\sigma_{\delta Be}$, $\sigma_{\delta S2S}$ and $\sigma_{\delta Wes}$). This allows the variation between different events, sites and paths to be compared to the variation between realisations, which also represents the simulation's uncertainty.

$$\Delta^k = a^k + \delta B_e^k + \delta S2S_s^k + \delta W_{es}^k \quad (2)$$

where Δ^k is the ground motion residual for each realisation k, a^k is the model bias (which also varies by realisation), δB_e^k is the between-event effects component with distribution $\sim N(0, \tau^k)$, $\delta S2S_s^k$ is the systematic site-to-site effects component with distribution $\sim N(0, \phi_{S2S}^k)$ and δW_{es}^k is the remaining within-event component with distribution $\sim N(0, \phi_{SS}^k)$.

3 RESULTS

3.1 Uncertainty results for a single event

Initially, comparisons were made between observed and simulated IMs on an event-by-event basis. Figure 4 provides this comparison for PGA and pSA(1.0s) for one event in the dataset. As uncertainties were included within the simulations, the simulated IMs are presented as a distribution which can be parameterised by a mean, standard deviation, and range for each record (as shown in Figure 4). We observe from these results that the simulated IM range at a number of sites does encompass the observation, which qualitatively indicates that the minimum amount of necessary input uncertainty has been included for those particular records. Approximately half of the sites also capture the observation within \pm one standard deviation (indicated by the solid grey line). However, a few sites do not meet either of these aims. It is also noted that there is no correlation between the simulation uncertainty and observation discrepancy, with the site distance or with the intensity measures for this particular event.

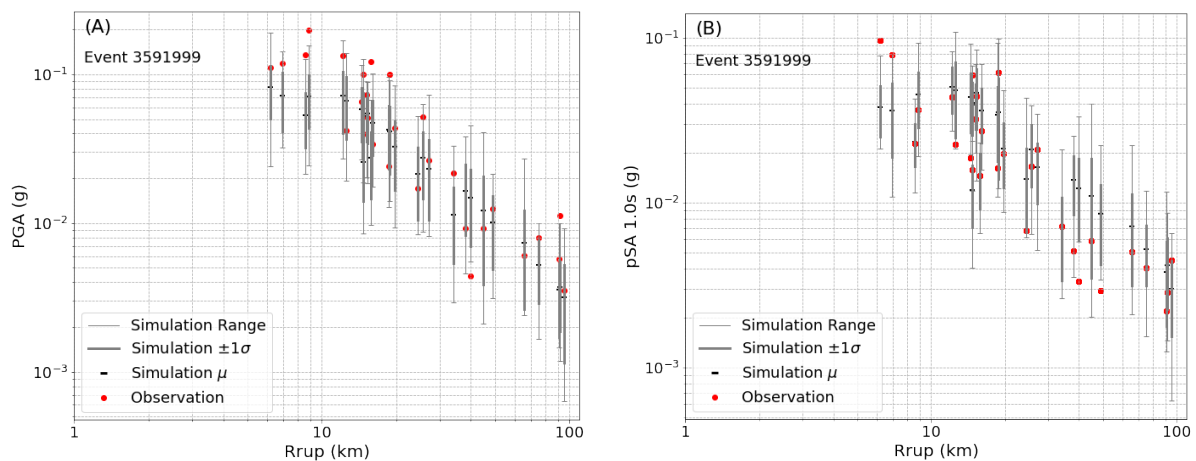


Figure 4: (A) PGA and (B) pSA 1.0s IMs with distance, for observations and simulations from event 3591999 and all recorded stations. If the model bias and uncertainty were sufficient, the observation would coincide with the simulation range for the majority of cases, which does not occur at all stations for these IMs.

3.2 Uncertainty results for all events

The main limitation of the procedure outlined in Section 3.1 is that each event must be assessed separately, making it difficult to understand overall trends and effects. In order to assess multiple events simultaneously, an approach was developed using normalised residuals (Z_p), as defined by Equation 3.

$$Z_p = \frac{\ln IM_{obs} - \mu_{\ln IM_{sim}}}{\sigma_{\ln IM_{sim}}} \quad (3)$$

where μ is the average of the simulated ground motion realisations for a single IM, event and station. σ is the standard deviation of the same. Z_p can be interpreted such that the simulations are unbiased if the average Z_p is equal to zero, and the target standard deviation for Z_p is 1 to indicate that an appropriate amount of uncertainty has been included in the simulations. Figure 5 demonstrates that σ_{Z_p} is approximately equal to 2 for most intensity measures, indicating the input uncertainties already considered are either too low and/or other model and parameter assumptions require explicit uncertainty consideration.

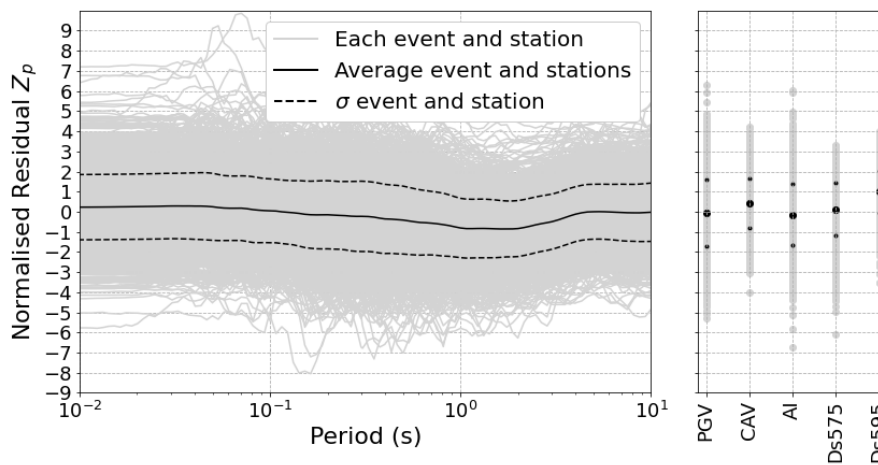


Figure 5: The normalised residual for all records across a number of intensity measures. These results show that for most events and sites at all intensity measures, more uncertainty is required, as $\sigma_{Z_p} > 1$.

3.3 Assessment of systematic effects

Assessing the normalised residuals is a useful tool for validation and the results can be compared with an equivalent analysis carried out using empirical ground motion models in order to set an acceptability threshold. However, this approach does not address the sensitivity of the uncertainty inputs with uncertainty outputs, nor does it indicate where further uncertainty is required.

In order to ascertain where more uncertainty is required, the systematic behaviour of the ground-motion residuals are assessed based on the equations in Section 2.4. Figure 6 shows the three component results for all response spectra intensity measures and all ground motion records. The variance components of each random effect and remainder terms are used to calculate the variation between events, sites and records (as shown in blue by τ , ϕ_{S2S} and ϕ_{SS} in Figure 6 (A), (B) and (C) respectively). These are computed for each realisation. The variance components of each random effect and remainder terms are also used to calculate the variation between realisations, for each event, site and record (as shown in red by $\sigma_{\delta Be}$, $\sigma_{\delta S2S}$ and $\sigma_{\delta Wes}$ in Figure 6 (A), (B) and (C) respectively). The mean and standard deviation of both distributions are shown in bold. These are compared (ie τ and $\sigma_{\delta Be}$, ϕ_{S2S} and $\sigma_{\delta S2S}$, and $\sigma_{\delta Wes}$ and ϕ_{SS}), in order to equate the difference in variation between the different events, sites or paths; with the variation between realisations (ie the simulation uncertainty). This would indicate whether the overall event, site and path uncertainties generated through the simulation method are sufficient for the systematic effect uncertainties intrinsic in the Canterbury

dataset. This aim is successfully achieved if the blue and red trend lines overlap. It can be observed from these results that the average and one standard deviation simulation uncertainties do not sufficiently achieve this aim, especially for site uncertainty and response spectra at short vibration periods. This is demonstrated by the solid and dashed red lines (variation between realisations) being lower than the solid and dashed blue (inherent variation between events, sites and paths). Further variance analysis into the components and their corresponding parameters would provide more detail as to the causative effects.

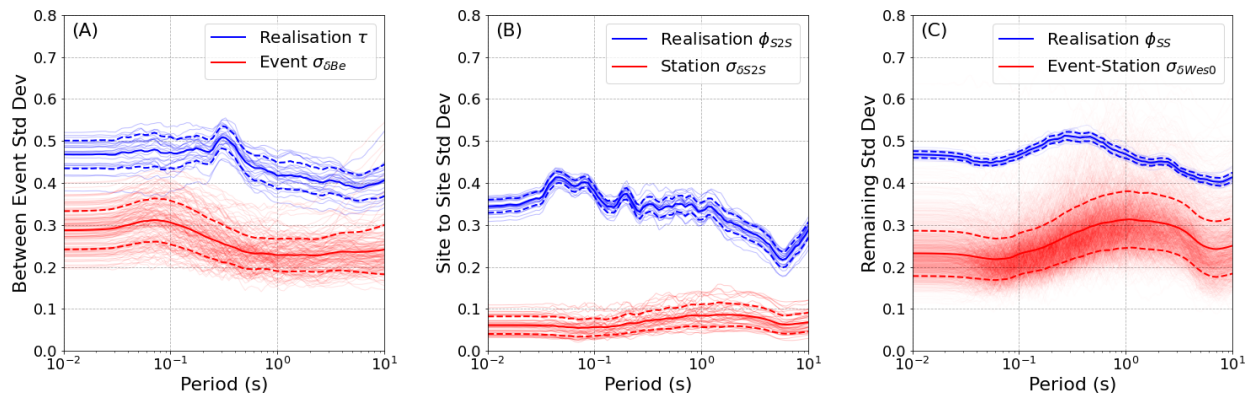


Figure 6: Ground motion residual effects for (A) between events, (B) site-site and (C) the remaining within-event. The realisation results (in blue) represent the variation between different events, sites or paths. The σ results (in red) shows the variation between realisations i.e. the input uncertainty. As these results do not show consistent overlap for all cases, the uncertainty is too low to capture the variation.

The possible reasons for the discrepancy between the input uncertainty and the inherent variation is either: that there is not enough uncertainty within the parameters considered; there are important uncertainty sources that have been neglected (such as other parameter uncertainties or factors); or there are shortcomings specific to the event, site or path parameters and models, as detailed below.

In the event component (Figure 6(A)) we see that the disparity is less apparent for very short and long periods (<0.1 and >4 seconds). This could indicate that more uncertainty is required in the stress parameter and/or rupture velocity, as they have a dominant effect on the corner frequency transition between the low and high frequency components of the model.

In Figure 6(B), it can be noted that the input site uncertainty is relatively low for short periods (<4 seconds). Vs30 measurement and calculation uncertainties have already been accounted for with the inputs of this study, however the site model uncertainty was not. Site model uncertainty can be added in future iterations, to account for uncertainty in the modified Campbell and Bozorgnia (2014) empirical site amplification model (de la Torre et al. 2016).

In Figure 6(C), the disparity between input uncertainty and inherent variation is most significant at short periods. A higher required HF path input uncertainty was expected, due to its simplified physics approach. Further refinements could be made to the attenuation uncertainty, as it is unlikely that these values should be the same in both the HF and LF methods. The prescribed shear wave velocity (V_s) uncertainty has also not yet been included, but is likely to be a significant contributor to path uncertainty. The V_s uncertainties in future iterations should be consistent across all velocity models.

4 CONCLUSION

The validation results show that some records have suitable input uncertainty for capturing the observational data (e.g. event 3591999 across most sites). However, the level of uncertainty is insufficient when assessed across all small magnitude Canterbury records at a number of intensity measures. Therefore, further

uncertainty input is required to account for additional parameter and modelling assumptions, simplifications and errors in the simulation model. In future iterations, it is planned to include inputs that account for the uncertainty in the selected site amplification model and the velocity model's shear wave velocities. It is also planned to make further refinements to the current model's anelastic attenuation uncertainty and the stress parameter uncertainty. Further variance analysis will also be undertaken to ascertain the performance of the uncertainties that are included, in order to make adjustments where required.

REFERENCES

- Bannister, S., Fry, B., Reyners, M., Ristau, J., & Zhang, H. 2011. Fine-scale Relocation of Aftershocks of the 22 February Mw 6.2 Christchurch Earthquake using Double-difference Tomography, *Seismological Research Letters*, Vol 82(6): 839-45.
- Boore, D.M., & Thompson, E.M. 2014. Path Durations for Use in the Stochastic-Method Simulation of Ground Motions Path Durations for Use in the Stochastic-Method Simulation, *Bulletin of the Seismological Society of America*, Vol 104(5): 2541-52.
- Campbell, K.W., & Bozorgnia, Y. 2014. NGA-West2 Ground Motion Model for the Average Horizontal Components of PGA, PGV, and 5% Damped Linear Acceleration Response Spectra, *Earthquake Spectra*, Vol 30(3): 1087-115.
- de la Torre, C., Bradley, B., & Lee, R. 2016. Modeling Nonlinear Site Effects in Physics-Based Ground Motion Simulations of the 2010-2011 Canterbury Earthquake Sequence, *Earthquake Spectra*, Vol.
- Eberhart-Phillips, D., Reyners, M., Bannister, S., Chadwick, M., & Ellis, S. 2010. Establishing a Versatile 3-D Seismic Velocity Model for New Zealand, *Seismological Research Letters*, Vol 81(6): 992-1000.
- Foster, K.M., Bradley, B.A., McGann, C.R., & Wotherspoon, L.M. 2019. A Vs30 Map for New Zealand based on Geologic and Terrain Proxy Variables and Field Measurements, *Earthquake Spectra*, Vol 0(0): null.
- Graves, R. 2018. "Personal Communication." In.
- Graves, R., & Pitarka, A. 2010. Broadband Ground-Motion Simulation Using a Hybrid Approach Broadband Ground-Motion Simulation Using a Hybrid Approach, *Bulletin of the Seismological Society of America*, Vol 100(5A): 2095-123.
- Graves, R., & Pitarka, A. 2015. Refinements to the Graves and Pitarka (2010) Broadband Ground-Motion Simulation Method, *Seismological Research Letters*, Vol 86(1): 75-80.
- Graves, R., & Pitarka, A. 2016. Kinematic Ground-Motion Simulations on Rough Faults Including Effects of 3D Stochastic Velocity Perturbations Kinematic Ground-Motion Simulations on Rough Faults, *Bulletin of the Seismological Society of America*, Vol 106(5): 2136-53.
- Graves, R.W., Aagaard, B.T., & Hudnut, K.W. 2011. The ShakeOut Earthquake Source and Ground Motion Simulations, *Earthquake Spectra*, Vol 27(2): 273-91.
- Lee, R.L., Bradley, B.A., Ghisetti, F.C., & Thomson, E.M. 2017. Development of a 3D Velocity Model of the Canterbury, New Zealand, Region for Broadband Ground-Motion Simulation Development of a 3D Velocity Model of the Canterbury, New Zealand, Region, *Bulletin of the Seismological Society of America*, Vol 107(5): 2131-50.
- Lee, R.L., Bradley, B.A., Stafford, P.J., Graves, R.W., & Rodriguez-Marek, A. 2019. Hybrid broadband ground motion simulation validation of small magnitude earthquakes in Canterbury, New Zealand, *Earthquake Spectra*, Vol.
- Lee, R.L., Bradley, B.A., Stafford, P.J., Graves, R.W., & Rodriguez-Marek, A. 2020. Hybrid broadband ground motion simulation validation of small magnitude earthquakes in Canterbury, New Zealand, *Earthquake Spectra*, Vol 36(2): 673-99.
- Mai, P.M., Spudich, P., & Boatwright, J. 2005. Hypocenter Locations in Finite-Source Rupture Models, *Bulletin of the Seismological Society of America*, Vol 95(3): 965-80.
- Neill, S.J., Lee, R.L., & Bradley, B.A. 2019. "Preliminary examination of kinematic rupture parameter variability in simulated ground motions." In *Pacific Conference on Earthquake Engineering*. Auckland, New Zealand.
- Ristau, J. 2008. Implementation of Routine Regional Moment Tensor Analysis in New Zealand, *Seismological Research Letters*, Vol 79(3): 400-15.
- Somerville, P., Sen, M., & Cohee, B. 1991. Simulation of strong ground motions recorded during the 1985 Michoacán, Mexico and Valparaíso, Chile earthquakes, *Bulletin of the Seismological Society of America*, Vol 81(1): 1-27.
- Taborda, R. 2015. "Evaluation of Attenuation Models (Q-Vs Relationships) used in Physics-Based Ground-Motion Earthquake Simulation through Validation with Data." In: SCEC.
- Thomson, E.M., Bradley, B.A., & Lee, R.L. 2019. Methodology and computational implementation of a New Zealand Velocity Model (NZVM2.0) for broadband ground motion simulation, *New Zealand Journal of Geology and Geophysics*, Vol: 1-18.